

A Gene of Many Functions:
Novel Roles for a Plant Epidermal Transcription Factor in Early Diverging Eudicots

Simra Zahid

A Thesis

Submitted in partial fulfillment of the
requirements for degree of

Master of Science

University of Washington

2021

Committee:

Verónica Di Stilio, Advisor

Takato Imaizumi

Adam Leache

Program Authorized to Offer Degree

Department of Biology

©Copyright 2021

Simra Zahid

University of Washington

Abstract

A Gene of Many Functions:
Novel Roles for a Plant Epidermal Transcription Factor in Early Diverging Eudicots

by
Simra Zahid

Chair of the Supervisory Committee: Verónica Di Stilio

Department of Biology

The epidermal transcription factors *MIXTA/MIXTA-like* modulate the differentiation of distinct cell identities in the epidermis of land plants. This study explored the evolutionary history and function of the *MIXTA-like* gene family in the early-diverging eudicot model *Thalictrum*. Phylogenetic analysis of the gene family revealed a lineage-specific duplication event that coincides with a Whole Genome Duplication (WGD) in the genus. In addition, *T. thalictroides* *MIXTA-like* gene was functionally characterized via targeted gene silencing, and a transcriptome analysis conducted to identify candidate targets. We found that *TthMYBML2* modulates leaf trichome morphogenesis through a microtubule-associated mechanism. Overexpression assays in a heterologous system (tobacco) provided further evidence for the leaf trichome function, while uncovering a novel role in the promotion of stigmatic papillae elongation. The latter finding, combined with the high differential expression of specific *MIXTA-like* paralogs in carpels of polyploid wind-pollinated *Thalictrum* suggests that *MIXTA-like* duplications may be implicated in the development of the long stigmatic papillae in the feathery stigmas of those species.

Table of Contents

1. Introduction.....	1
2. Results.....	6
3. Discussion.....	22
4. Methods.....	25
5. References.....	30
6. Supplementary data.....	38

Acknowledgements

This work was funded by NSF DEB-1911539 to VSD and the Hall International Fellowship (University of Washington, UW) to SZ. S.Z is thankful for the Lawrence Giles and Kruckeberg-Walker Awards (UW). We thank Wai Pang Chang for his help in the preparation and observation of samples in the JEOL NeoScope JCM-7000, funded by the Student Technology Fee (STF). Stephanie Ickert-Bond (U. of Alaska) provided *T. sparsiflorum* specimens. Jens Johnson and Valerie Soza started the *Thalictrum MIXTA-like* alignment. We thank Cathie Martin for the transformed tobacco materials.

Introduction

Plants have evolved various epidermal features for environmental adaptation (Javelle et al., 2011). In fact, epidermal cell types are useful micromorphological markers to differentiate between different types of plant organs (Speisser et al., 2021). In land plants, MYB genes make up the most prominent family of transcription factors with varying numbers of contiguous repeats (one-four). Most plants encode the R2R3 MYB genes with two repeats functioning in secondary metabolite production and cell identity (Stracke et al., 2014). A subgroup of the R2R3 MYB protein subgroup 9A *MIXTA/MIXTA-like* gene family (Brockington et al., 2013) has specialized roles in epidermal cells (see Table. 1 for full details), including conical cells (Noda et al., 1994; Baumann et al., 2007, Di Stilio et al. 2009), trichomes (Jakoby 2008; Yan et al., 2018; Qin et al., 2021), and cotton fibers which are specialized ovule epidermal cells (Machado et al., 2009), and more recently in the cuticle (Lashbrooke et al., 2015; Lu et al., 2021). In fact, some *MIXTA-like* genes have evolved multiple functions in epidermal cell patternings, such as regulating trichome branching and conical cells by *Antirrhinum majus AmMYBML1* (Perez-Rodriguez et al., 2005). At present, most of the functional information on *MIXTA/MIXTA-like* genes comes from studies done in core eudicot clade (Brockington et al., 2013). In contrast, there is a gap in knowledge about the function of R2R3 S9-A genes in epidermal fate in early-diverging eudicots. Within the monocots, the *MIXTA-like* ortholog of the orchid *Dendrobium crumenatum DcMYBML1* is capable of rescuing the branched trichome phenotype of *Arabidopsis thaliana noeck* mutants (Gilding and Marks, 2010), even though it does not produce trichomes in the orchid. Given this complexity, additional functional studies of *MIXTA-like* genes are needed in early-diverging plant species to reconstruct the ancestral gene function in this important gene family.

Trichomes or epidermal hair can be classified as either non-glandular or glandular (Feng et al., 2021). For plants, non-glandular trichomes have adaptive value as they provide protection

against UV-B radiation and dehydration, while glandular trichomes are warehouses of valuable defense metabolites, such as sclareol and artemisinin, which protect plants against herbivores (Chalvin et al., 2021; Yan et al., 2018). In addition, trichomes are a great model for studying single-cell differentiation as they are structurally simple and easily accessible (Yang & Ye, 2012). On the one hand, differentiation of unicellular trichomes in *A. thaliana* is well understood, being controlled by an activation-inhibition loop (Jakoby et al., 2008). The positive regulators GLABRA3 (GL3), GLABRA1 (GL1), TRANSPARENT TESTA GLABRA1 (WD40) form a trimeric complex with basic helix-loop-helix proteins (bHLH) (MYB-bHLH-WD40) that stimulates trichome differentiation in the epidermis (Pesch et al., 2009). In the surrounding cells, transcription factors such as TRIPTYCHON (TRY) and TRICHOMELESS1,2 (TCL1 and TCL2) bind and inactivate the bHLH-WD40 complex, thereby suppressing trichome development (Gao et al., 2021). The regulatory network for multicellular trichomes, on the other hand, is less clear, with HD-ZIP IV transcription factors known to interact with MIXTA-like orthologs during trichome development in corn, cucumber, and sweet wormwood (Vernoud et al., 2009; Wang et al., 2015; Yan et al., 2018), while a B type cyclin plays this role in tomato (Gao et al., 2017). Hence, further investigation of multicellular trichome development and the underlying genetic regulators is warranted.

Thalictrum (meadow-rue) are herbaceous perennials in the buttercup family Ranunculaceae, in the non-core eudicots that contain a diversity of medicinal compounds, such as berberine and magnoflorine produced in their roots and leaves (Bhakuni & Singh, 1982, Alhowiriny, 2002). The *Thalictrum* MIXTA-like ortholog *TthMYBML2* plays a role in conical cell development in floral organs (petaloid sepals and showy stamen filaments), potentially connected to insect pollination. *TthMYBML2* is highly expressed in carpels in the stigmatic papillae (Di Stilio et al., 2009), but its role in vegetative leaves remains unknown.






Here, I set out to examine the function of a MIXTA-like ortholog in the leaves of the early diverging eudicot *Thalictrum thalictroides*, where the developmental genetics of epidermal

features is unknown. This study has the potential to shed light on the reconstruction of ancestral gene function for this important family of plant epidermal transcription factors. The specific goals of this study are to

1. Reconstruct the evolutionary history of *MIXTA-like* genes in *Thalictrum* species with diverse ploidy, sexual system and pollination mode;
2. Compare tissue-specific expression patterns between a diploid, a tetraploid, and a high level polyploid to investigate the potential role of gene duplication on gene function;
3. Investigate gene function of the *Thalictrum Mixta-like* ortholog in leaves of diploid *T.thalictroides* via targeted gene silencing and heterologous overexpression in tobacco;
and
4. Perform comparative transcriptome profiling of leaves targeted for gene silencing to identify candidate genes and to work towards eventually elucidating its gene regulatory network (GRN).

In summary, this study provides functional information for *Mixta-like* genes in the leaves of an early diverging eudicot to better understand the underlying molecular mechanisms in trichome development and cell differentiation.

Table 1: Summary of functional data currently available for R2R3 MYB orthologs (subgroup 9) in epidermis across various plant systems. Orthologs in bold have multiple functions. *A. majus*=*Antirrhinum majus* (snapdragon); *G. hirsuta*= *Gossypium hirsutum* (cotton), *P. hybrida*=*Petunia hybrida*; *A. thaliana*= *Arabidopsis thaliana* (thale cress); *P. trichopoda*= *Populus trichopoda* (poplar); *T. thalictroides* = *Thalictrum thalictroides* (meadow-rue); *M. truncatula*= *Medicago truncatula* (clover); *D. crumenatum*= *Dendrobium crumenatum* (orchid); *D. hybrida*= *Dendrobium hybrida* (orchid). *polymorpha*= *Marchantia polymorpha* (liverwort); *P. aphrodite* = *Phalaenopsis aphrodite* (orchid); *S. lycopersicum* = *Solanum lycopersicum* (tomato); *A. annua* = *Artemisia annua* (sweet wormwood); *M. guttatus* = *Mimulus guttatus* (monkey flower). Full references are listed in the bibliography.

Species	Gene	Tissue	Reference	Function (Positive regulation)
<i>A. majus</i> , <i>P. hybrida</i> , <i>A. thaliana</i> , <i>T. thalictroides</i> , <i>P. aphrodite</i> , <i>D. hybrida</i>	<i>AmMIXTA</i> , <i>AmMYBML1</i> , <i>AmMYBML2</i> , <i>AmMYBML3</i> , <i>PhMYB1</i> , <i>AtMYB16</i> , <i>TtMYBML2</i> , <i>PaMYB9A1/2</i> , <i>DhMYB1</i> ,	Petals/sepals	Noda et al., (1994), Perez-Rodriguez et al., (2005), Baumann et al., (2007), Jaffe et al., (2007), Di Stilio et al., (2009), Lau et al., (2015), Lu et al., (2021)	Conical cell development 
<i>A. majus</i> , <i>G. hirsuta</i> , <i>P. trichopoda</i> , <i>A. annua</i> , <i>D. crumenatum</i> , <i>M. truncatula</i>	<i>AmMYBML1</i> , <i>GhMYB25</i> , <i>PtMYB186</i> , <i>MtMYBML3</i> , <i>DcMYBML1</i> , <i>AaMYB17</i>	Leaves/petals	Perez-Rodriguez et al., (2005), Machado et al., (2009), Plett et al., (2010), Gilding and Marks (2010), Qin et al., (2021)	Trichome development 
<i>M. polymorpha</i> , <i>P. aphrodite</i> , <i>S. lycopersicum</i> , <i>A. thaliana</i>	<i>MpSBG9</i> , <i>PaMYB9A1/2</i> , <i>SIMIXTA</i> , <i>AtMYB106</i> , <i>AtMYB16</i>	Gametophyte thallus, petals, fruit, leaves	Gilding and Marks (2010). Lashbrook et al., (2015), Xu et al., (2021), Lu et al., (2021)	Cuticle biosynthesis 
<i>G. hirsuta</i>	<i>GhMYB25</i> , <i>GhMYB25-like</i>	Ovules	Machado et al., (2009), Walford et al., (2011)	Cotton fiber initiation (on the ovule epidermis) 
				Function (Negative regulation)
<i>A. thaliana</i> , <i>M. guttatus</i> , <i>S. lycopersicum</i>	<i>AtMYB106</i> , <i>MgMYBML8</i> , <i>SIMIXTA</i>	Petals, leaves	Gilding and Marks (2010), Scoville et al., (2011), Galdon-Armero et al., (2020)	Trichome initiation 

Results

An early duplication in the *Thalictrum* MIXTA-like genes coincides with a genus-wide whole genome duplication event

A phylogenetic approach was used in order to understand the evolutionary history of the *MIXTA-like* gene clade in *Thalictrum* (Ranunculaceae). To this end, a nucleotide alignment was constructed for 52 SBG9-A sequences isolated from 24 species spanning the two major clades in *Thalictrum* (Martínez-Gómez et al., in prep, Wang et al., 2019) and identified based on the conserved R2R3 domains and a highly conserved Subgroup 9A domain (Suppl. Fig. 1). A consensus phylogenetic tree was inferred using the Bayesian optimality criterion implemented in MrBayes (Fig. 1b). Two *MIXTA-like* SBG9-A sequences from *Aquilegia formosa* (Ranunculaceae) were used as an outgroup, to root the tree. The results indicate that *MIXTA-like* SB9-A sequences group into two distinct clades with strong support, clade I (*ThMYBML2*) named after the first *MIXTA-like* gene analyzed from *T. thalictroides*, and Clade II with subclades *ThMYBML2-a* and *ThMYBML2-b*. Based on these findings, a gene duplication event was inferred at the base of the two subclades, as paralogs from polyploid species were distributed between the two clades (see representatives in bold, Fig. 1b). One of the paralogs from the tetraploid species *T. arsenii* was sister to clade II. On closer inspection, the sequence alignment for this paralog reveals a lower conservation of nucleotides in the intron regions.

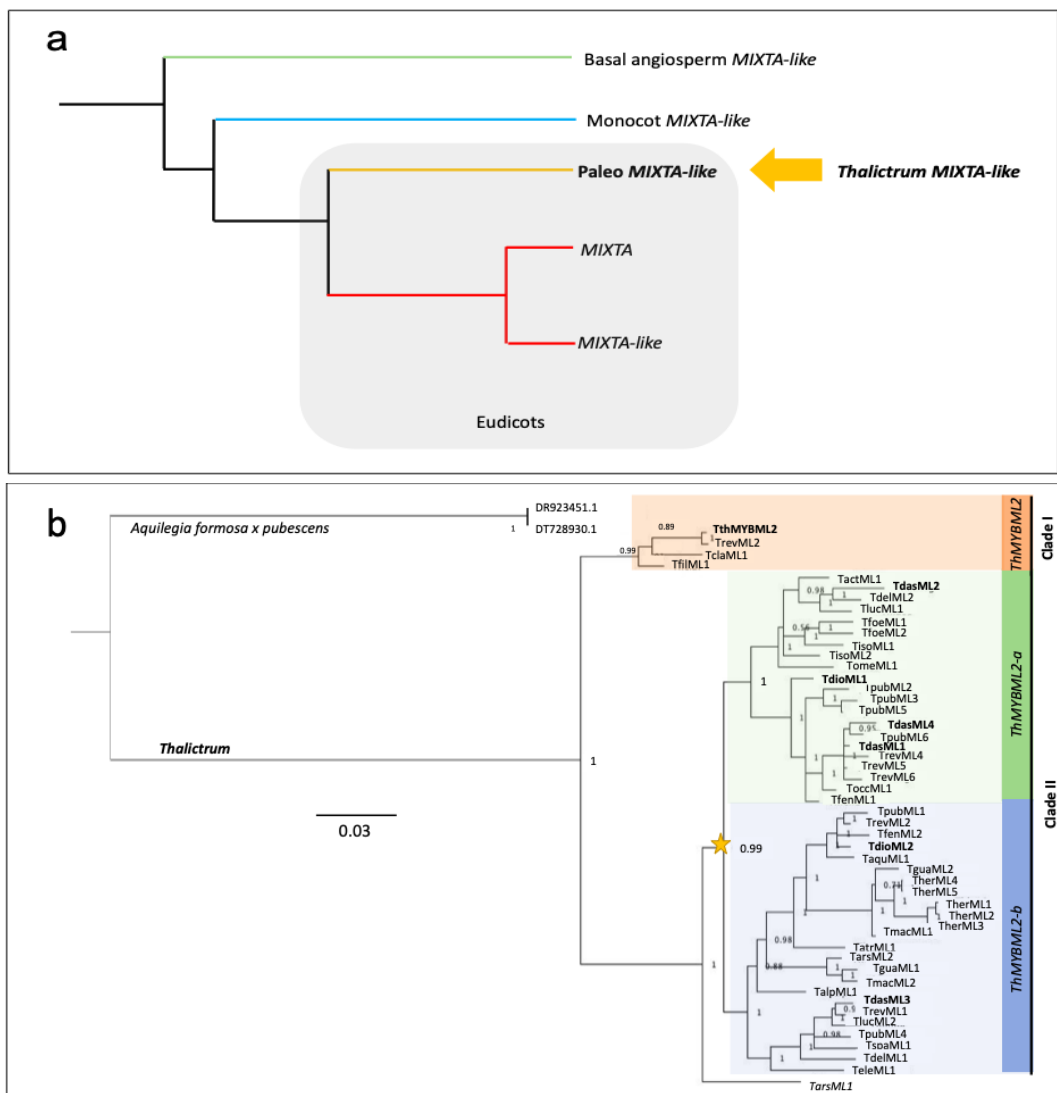


Figure. 1: Gene phylogeny of *Thalictrum* MIXTA-like orthologs. (a) Simplified tree of the *MIXTA/MIXTA-like* gene family in angiosperms. Organismal coding: green= ANITA grade; blue= monocot; yellow= basal early diverging eudicots; red= core eudicot. (b) Bayesian Inference phylogeny using *Aquilegia formosa x pubescens* (Ranunculaceae) as an outgroup reveals two major clades I (orange), and two subclades, *ThMYBML2a* (green) and *ThMYBML2a* (blue), within clade II. Numbers next to nodes are posterior probabilities. The star indicates an inferred gene duplication event. Branch lengths indicate substitutions per site. Bolded genes were the subject of this study.

Specific *MIXTA-like* gene copies are highly expressed in *Thalictrum* carpels and female flowers

To test the spatial expression patterns of *MIXTA-like* homologs, qPCR was performed on leaves and dissected floral organs (sepals, carpels, and stamens) of young open flowers, since this is when expression is known to peak in other species (Perez Rodriguez 2005, Lau et al., 2015, Lu et al., 2021). We chose three representative species, *T. thalictroides*, *T. dioicum*, and *T. dasycarpum* (Table. 2): *Thalictrum thalictroides* is a diploid species with the ancestral traits of insect-pollinated, hermaphrodite flowers, whose petaloid sepals contain conical cells. In contrast, *T. dioicum* (4x) and *T. dasycarpum* (21x) are wind-pollinated polyploids with small and inconspicuous unisexual flowers that contain long pendulous stamens and feathery stigmas.

Table2. Ploidy level, pollination mode and sexual system for *Thalictrum* species in this study.

Species	Ploidy Level	Pollination mode	Sexual system
<i>Thalictrum thalictroides</i>	Diploid (2X)	Insect	Hermaphrodite
<i>Thalictrum dioicum</i>	Polyploid (4X)	Wind	Unisexual (dioecious)
<i>Thalictrum dasycarpum</i>	Polyploid (21X)	Wind	Unisexual (dioecious)

There was a trend towards high *ThMIXTA-like* expression for specific orthologs in the carpels of the three species, and female leaves and sepals of *T. dioicum* and *T. dasycarpum* respectively (Fig. 2). Stamens, and most male tissues from all three species showed a lower combined relative expression. In *T. thalictroides*, *ThMYBML2* showed highest expression in carpels, followed by sepals and leaves (Fig. 2a). Similarly, both paralogs from *T. dioicum* (*TdioML1* and *TdioML2*) showed high carpel-specific expression, suggesting partial redundancy in function (Fig. 2b). In *T. dasycarpum*, the paralog *TdasML4* showed high expression in the carpels suggesting functional specialization in carpel epidermis (Fig. 2c). However, *TdasML2* showed

higher expression in stamens than the other homologs. On closer inspection, the R2 and R3 MYB domains of the lowest expressing copies (*TdasML1* and *TdasML3*) showed two single amino acid substitutions, K43N and S76N (Suppl. Fig.1). Single amino acid mutations in the R2R3 domains cause loss of promoter-site interactions that result in downregulation of expression for other MYB proteins (Hichri et al., 2011; Dai et al., 2016). Taken together, specific *MIXTA-like* genes show a sex-dependent expression pattern in *Thalictrum* and, while some species like *T. dioicum* show redundant expression of paralogs, others like *T. dasycarpum* show a more specialized expression pattern.

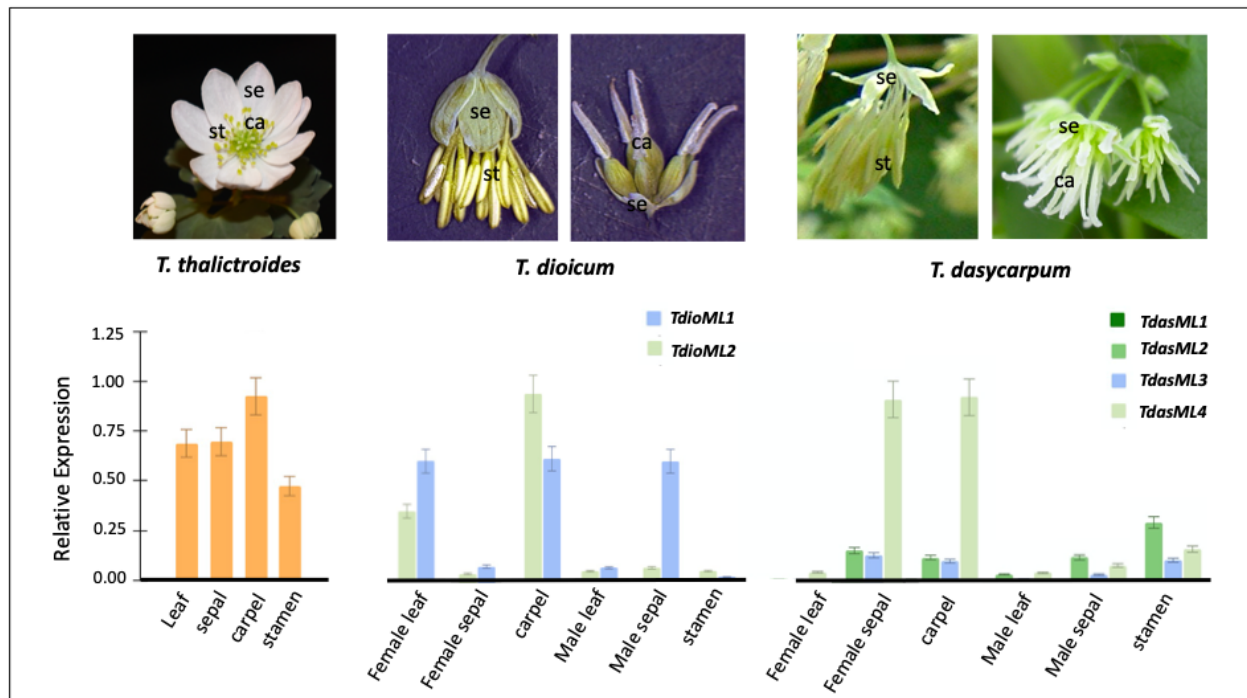


Figure. 2: Relative expression of *Thalictrum MIXTA-like* in leaves and floral tissues.

Hermaphrodite flowers of *T. thalictroides* (left), staminate and carpellate flowers of *T. dioicum* (middle) and *T. dasycarpum* (right). Quantitative RT-PCR showing average expression ($2^{-\Delta\Delta Ct}$) of *Thalictrum MIXTA-like* relative to the housekeeping genes *ThtACTIN* and *ThEEF1-alpha*,

normalized to the highest expressing paralog. Color coding matches the gene lineages shown in Fig. 1b. Error bars represent \pm standard error of the mean. N= 4-7 flowers.

Targeted silencing of *TthMYBML2*

In order to understand the function of an early diverging eudicot *MIXTA-like* ortholog in leaves, *TthMYBML2* was targeted for downregulation by VIGS. Mock-treated plants were indistinguishable from untreated wild type plants, except for previously described background effects, such as necrotic lesions (Fig. 3a, d-g). The infection efficiency was 35%, with fifteen out of forty-five plants showing a range of photobleaching 3-4 weeks post infiltration (Fig. 3b, c, g).

Viral transcripts were detected in the treated plants and their gene expression was validated (Fig. 4). Two transcripts of the bipartite viral system, TRV1 and TRV2, were found in mock treated and treated lines, confirming a successful infiltration (Fig. 4a). There was an 11.1 fold decrease in the average expression of *TthMYBML2* compared to empty vector controls (Fig. 4b). Variegated and photobleached leaves in TRV2-*PDS-ML2* treated plants showed correlated downregulation of *TthMYBML2* and *TthPDS* (Fig. 4b), confirming that both the reporter and target genes were silenced together, as intended.

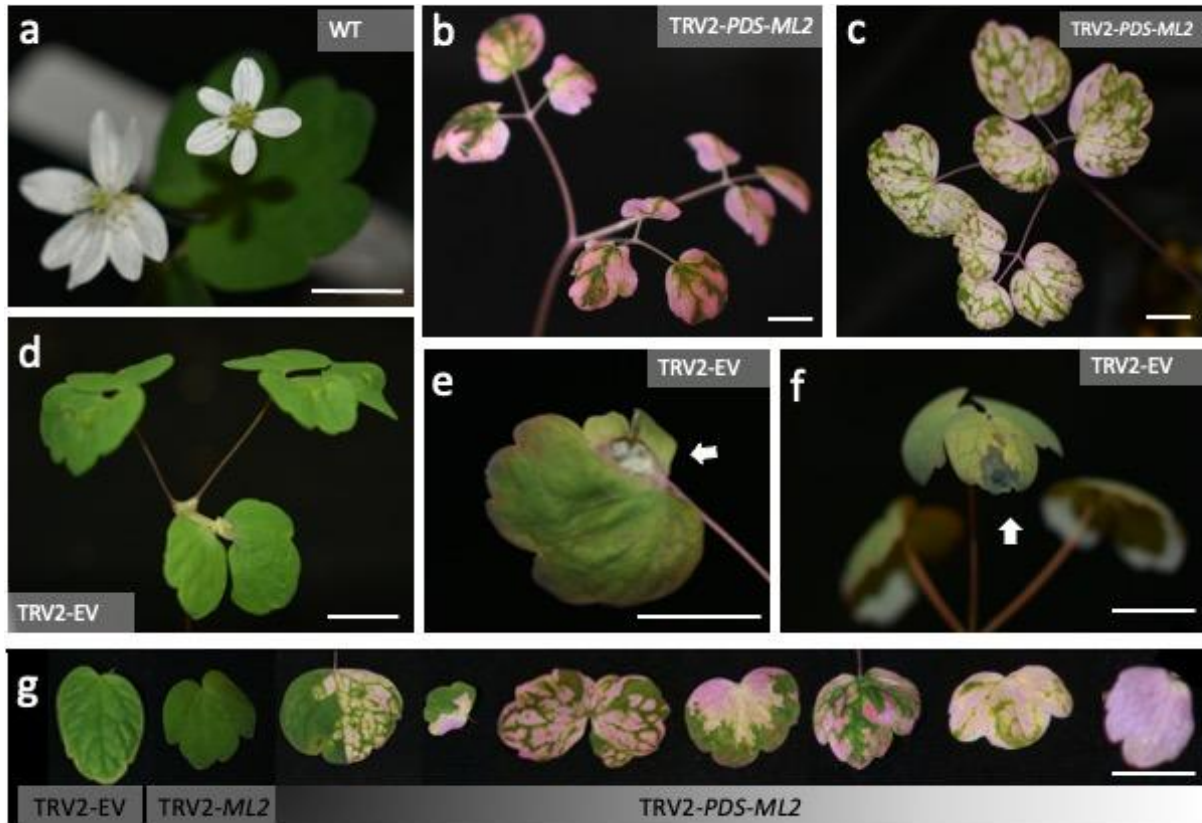


Figure 3: Virus Induced Gene Silencing (VIGS) of a *MIXTA-like* gene from the early diverged basal eudicot *T. thalictroides* (Ranunculaceae). (a) Untreated control (b-c) TRV2-*PDS-ML2* treated plants showing photobleaching of leaf tissue. (d-f) Mock (empty TRV2) treated plants, arrows show background viral effects. (g) Leaf profiles of treated groups, from left to right: mock controls, TRV2-*ML2*, and TRV2-*PDS-ML2* showing a range of photobleaching resulting in variegated leaves. Scale bars: 10 mm.

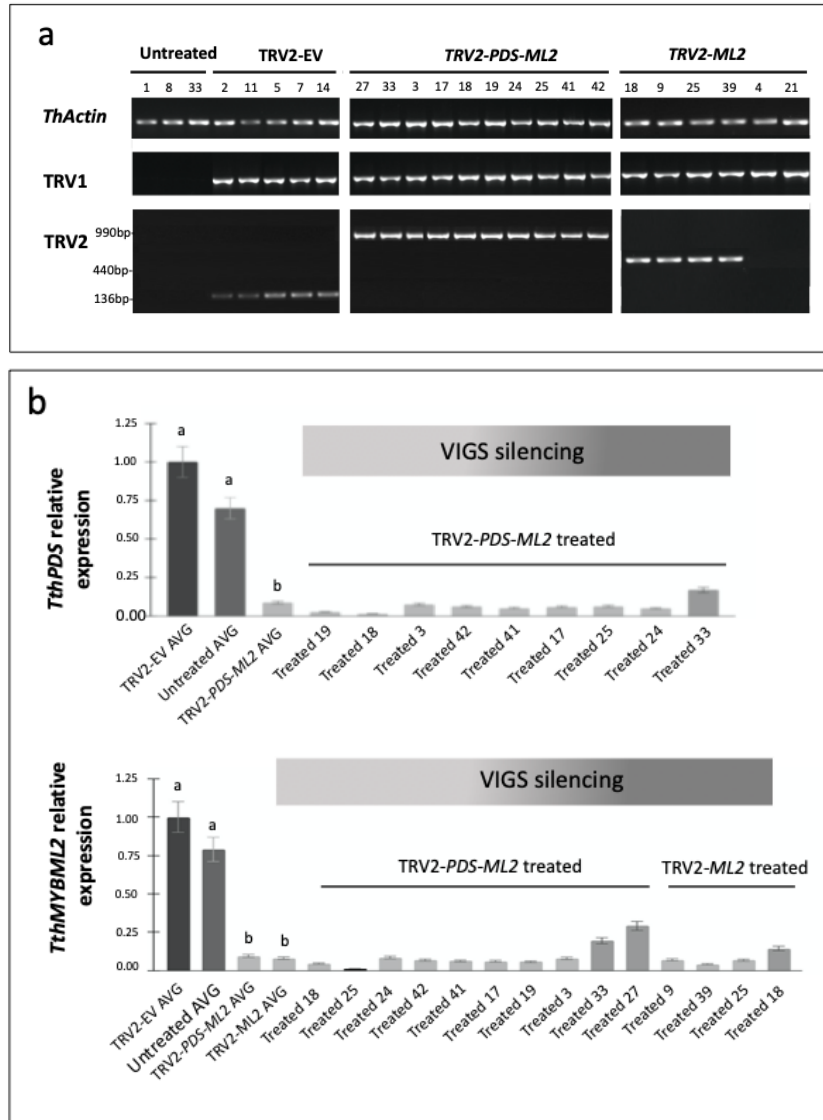


Figure 4: Molecular validation of targeted silencing of *TthMYBML2* by VIGS in *T. thalictroides*. (a) Reverse Transcriptase (RT-PCR) using locus specific primers to detect viral transcripts in TRV2-EV and TRV2-ML2, TRV2-PDS-ML2 lines. The housekeeping gene *TthActin* was used as a loading control. Viral transcripts were only detected in treated lines. Approximate band size indicated for TRV2, larger bands result from the presence of the targeted gene insert. (b) Gene expression molecular validation by qPCR for the expression *TthMYBML2* and *TthPDS*, normalized to empty vector controls. Expression is relative to *TthACTIN* and *TthEEF1* standards.

*One way ANOVA, different letters alphabets indicate significant differences by Tukey's comparison test ($p= 0.008$). Error bars represent \pm standard error of the mean. Plants in bold were used in a followup RNA-seq experiment.

Targeted gene silencing reveals a novel role for an early-diverging eudicot *MIXTA*-like in trichome morphogenesis in leaves

To establish the role of *TthMYBML2* in leaves, epidermal features such as trichomes, stomata, and pavement cells were evaluated on the adaxial and abaxial side of the leaves from down-regulated and mock treated *T. thalictroides* plants. In this species, trichomes can develop on the underside of the leaves (Fig. 5a-c), as well as on the floral organs(not shown). Scanning electron microscopy (SEM) revealed that trichomes from the mock treated controls were indistinguishable from those in untreated leaves, consisting of a stalk and a head (capitate trichomes, Fig. 5a-c). In contrast, trichomes from treated plants showed a “stubby”, short stalk phenotype (Fig. 5d,e,g). In fact, trichomes from certain treated plants undergoing targeted gene silencing resembled either conical cells (Fig. 5d), or showed an irregular appearance (Fig. 5h, Suppl. Fig. 5.), or micro trichomes (Fig. 5f).

To further confirm the trichome phenotype, we compared sectors of photobleached and green tissues within variegated leaves (Fig. 3g). As expected, green leaf sectors had taller trichomes than the short stubby trichomes in photobleached sectors (Fig. 5i, Suppl. Fig. 3). Average trichome height in treated plants was 2.7 fold shorter than mock treated controls, and this effect was statistically significant ($N= 41$, $p \leq 0.0001$ (Fig. 5j). Taken together, these results suggest that the *T. thalictroides* *MIXTA*-like ortholog plays a role in cell elongation and morphogenesis of leaf trichomes.

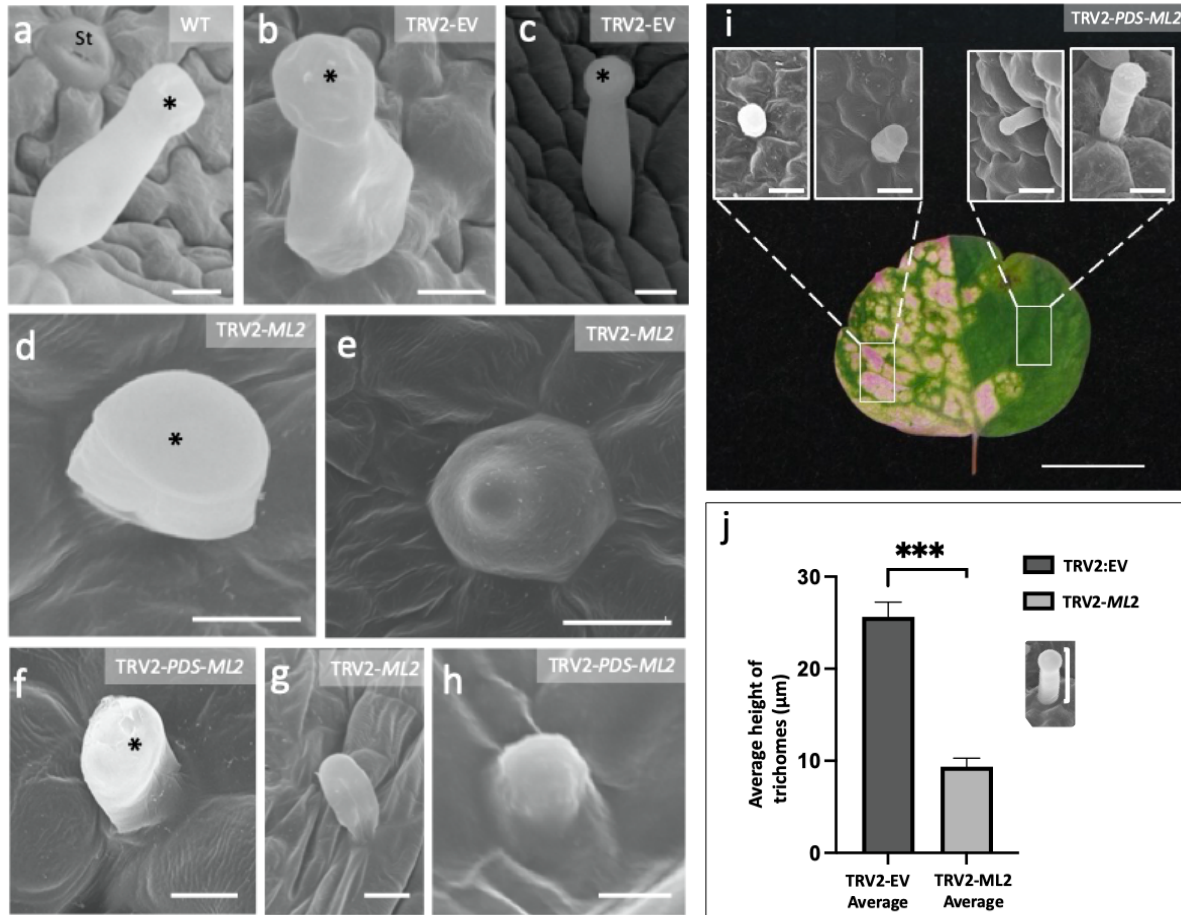


Figure 5: Targeted silencing of a *Thalictrum MIXTA-like* affects trichome morphogenesis.

Comparison of trichomes found in leaves of mock treated and VIGS-treated plants by SEM. (a, b, c) trichome phenotypes from mock-treated and mature wild type plants. Asterisks indicate the position of the trichome head in these capitate, glandular trichomes. (d, h) “Stubby” trichomes in *TthMYBML2* down-regulated lines representing at least three independent lines. (i) Trichome phenotypes from either green or photobleached sectors within variegated leaves. Rectangles show areas where the trichomes were sampled. (j) Quantitative difference in trichome cell height, measured as diagrammed on the inset (N=41). Averages \pm SE, asterisk indicates statistical significance between group means ($P \leq 0.0001$). Scale bars in (a-e, g-h) = 10 μ m, and (f) = 2 μ m.

No significant differences were found in the morphology of pavement cells (Fig. 6a-f) or the mean stomatal densities between mock treated and *TthMYBML2* down regulated plants (Fig. 6g,h,j); however, independent down-regulated plants showed variations in stomatal densities across the top, middle, and bottom leaf abaxial sections (Fig. 6j).

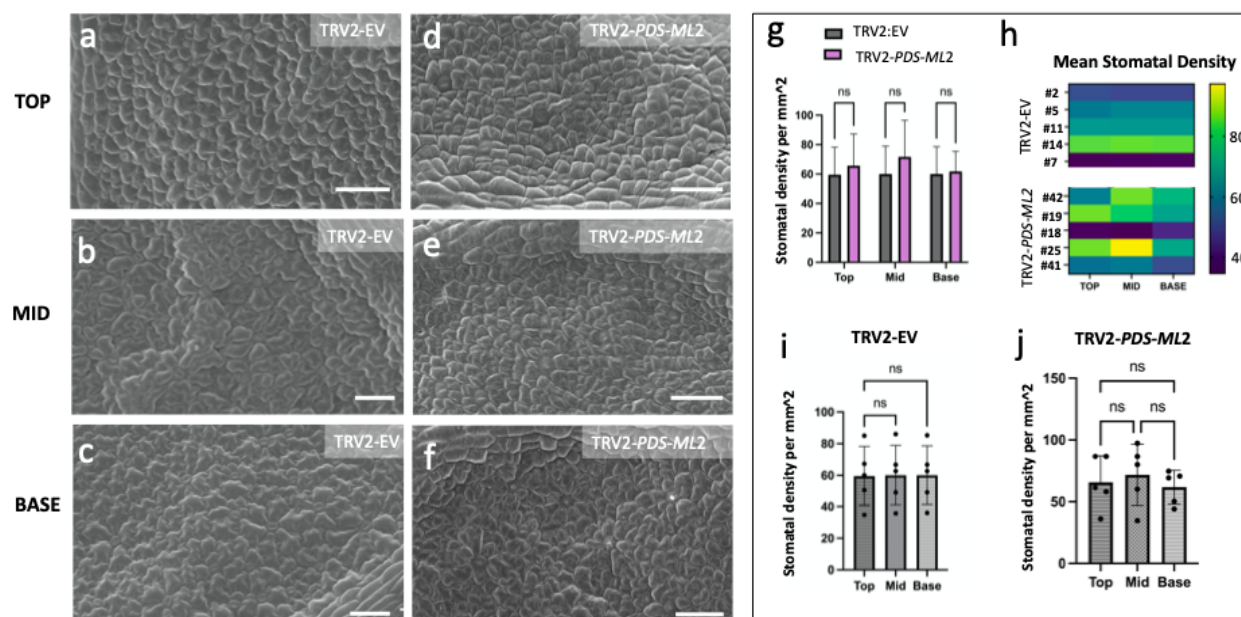


Figure 6: *Thalicttrum MIXTA-like* does not affect Stomatal density. SEM of abaxial top, middle and base regions of leaves treated by VIGS and controls: (a-c) mock-treated leaves (empty vector control); (d-f) Leaves undergoing silencing of *TthMYBML2*. (g,h) Mean stomatal density per mm² across the leaf landscape. (i) Heat map showing mean stomatal density at the top, middle, and base leaf sectors for five independent transgenic plants. (j) Stomatal densities per mm² in mock treated and VIGS plants. Data represented are means \pm SE (n = 5). Scale bars in (a-j) = 50 μ m.

Heterologous overexpression of *Thalictrum MIXTA-like* induces ectopic, branched trichomes

At present, a functional approach for overexpression in *Thalictrum* is unavailable. To conduct a complementary test, heterologous overexpression was pursued using an established bioassay in tobacco (Di Stilio et al., 2009), and fixed leaves from that experiment were used here for observations of epidermal features under SEM. In the tobacco family *Solanaceae*, glandular, non-glandular and defense trichomes are found (Bar and Shtein, 2019). Two types of non-glandular (Type I, II), glandular (III, IV) and one type of defense trichome (Type V) were identified on the upper and lower surface of wild type tobacco leaves (Fig. 7a-e).

Transgenic lines overexpressing *TthMYBML2* had ectopic branched trichomes (arrows, Fig. 7f-h), a higher type II trichome density on the adaxial side, and type I, II, IV, and V trichome density on the abaxial side (Fig. 7k). Moreover, the abaxial stamen epidermis showed ectopic development of both conical cells and trichomes in transgenic plants (Fig. 8b,d). Taken together, these findings suggest that *TthMYBML2* is a positive regulator of trichome development and can direct the differentiation of multiple epidermal features.

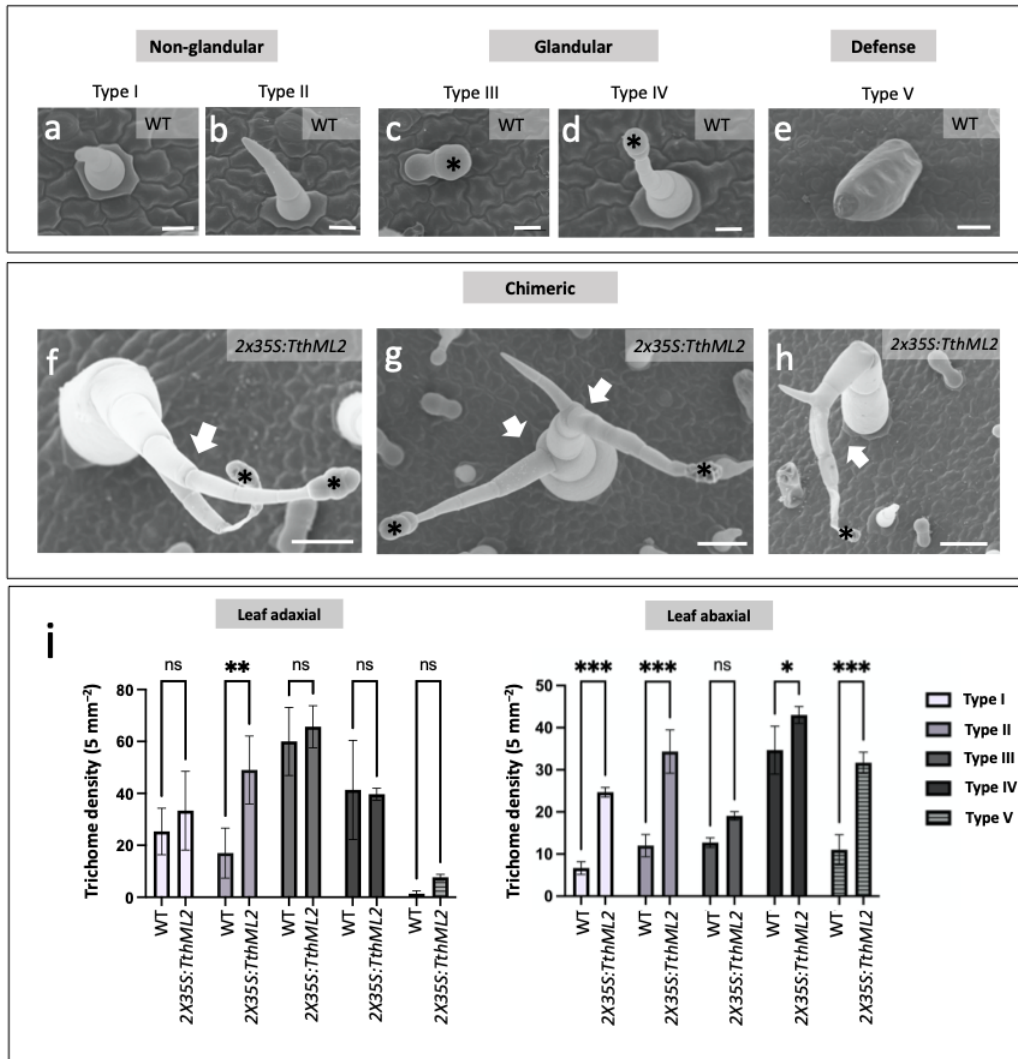


Figure 7: Overexpression of *TthMYBML2* leads to ectopic and abnormal trichomes in tobacco leaves. (a-e) Trichome types (I-V) identified on the leaves of wild type tobacco. Asterisks indicate the position of the glandular head of capitate trichomes. (f-j) Ectopic branched trichomes on the transgenic tobacco leaflets, arrows show branching. (i) Average density of trichome types per 5 mm² on the adaxial (left) and abaxial (right) side of the leaves of transgenic versus wild type tobacco plants. Averages \pm SE shown. Asterisks indicate significant differences in trichome counts in a two-way ANOVA with Bonferroni correction for multiple comparisons: * $P < 0.05$; ** $P < 0.01$, *** $P < 0.001$. Scale bars in (a-j) = 50 μ m.

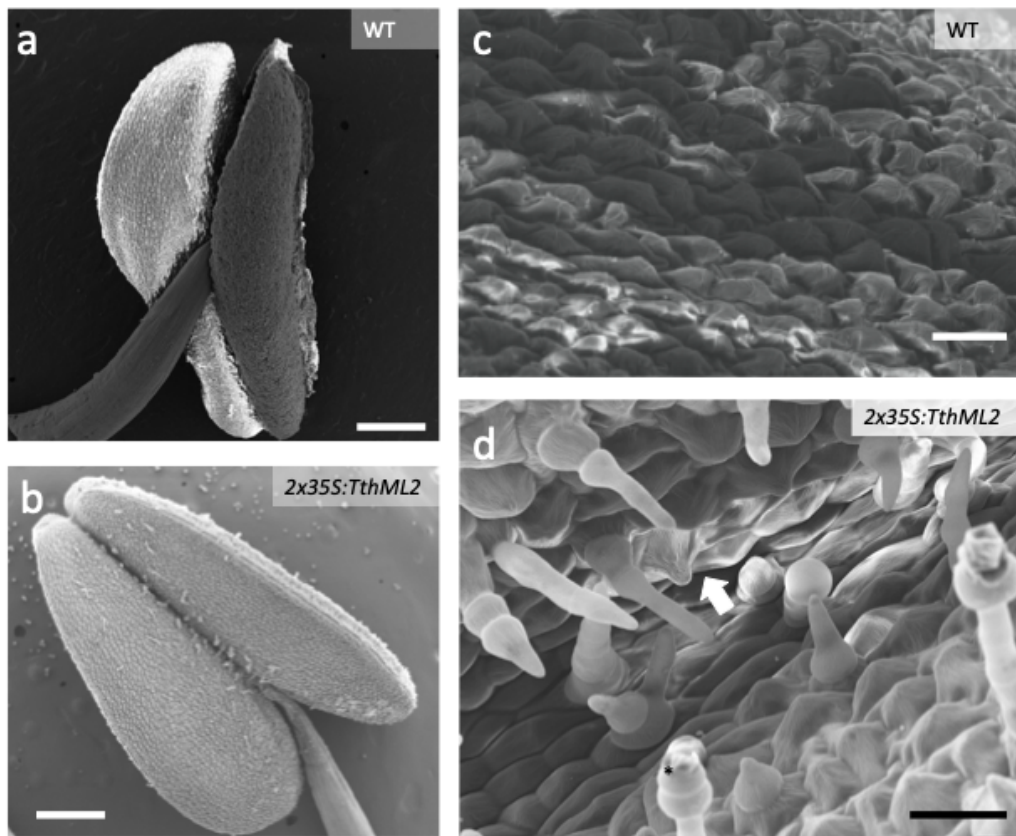


Figure 8: *Thalictrum Mixta-like2* induced development of ectopic trichomes and conical cells on the epidermis of stamens. Scanning electron micrographs of stamens showing the abaxial epidermis of an anther of (a,c) wild type tobacco, and (b, d) transgenic tobacco. The white arrow indicates ectopic conical cells, the asterisk a trichome head. Scale bars: a, b =500 μm ; c, d= 50 μm .

Overexpression of *Thalictrum MIXTA-like* induces cell elongation in stigmatic papillae

Given that *TthMYBML2* is expressed in the stigmas of *T. thalictroides* carpels (Di Stilio et al., 2009), we tested whether its overexpression could induce stigmatic papillae cell elongation in the tobacco bioassay. Tobacco stigmas are “wet”, covered in secretions that function in

pollen-mediated interactions (Hscock & Allen, 2008); therefore, only sectors free of the exudate could be sampled (Fig. 9a-e). Stigmatic papillae from overexpressing plants showed a twenty percent increase in cell length compared to those from wild type tobacco (Fig. 9f). This data suggests that *TthMYBML2* is a positive regulator of cell length in stigmatic papillae, a novel role described here for this gene family.

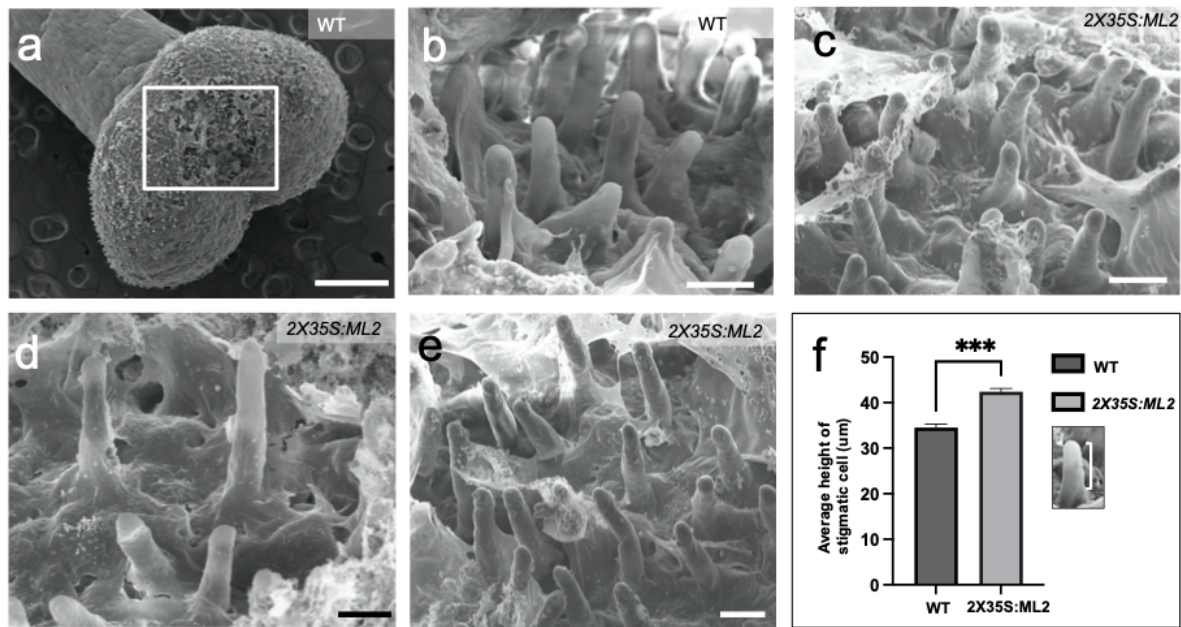


Figure. 9: Overexpression of *Thalictrum MIXTA-like* induces stigmatic papillae elongation in tobacco. (a) SEM of a tobacco stigma, the rectangle indicates the area free of exudate that was analyzed. (b) Stigmatic papillae of wild type tobacco. (c-e) Stigmatic papillae of transgenic tobacco overexpressing the *Thalictrum MIXTA-like* ortholog. (f) Average height of stigmatic papillae in wild type and transgenic tobacco carpels, measured as diagrammed in inset (N=145, 7 independent transgenic lines). Averages \pm SE, asterisks indicate a statistical significant difference between the means ($p < 0.001$). Scale bars (a) 500 μm , (b-e) 30 μm .

Identification of candidate genes in the leaf gene regulatory network of paleo MIXTA-like

To determine the molecular mechanisms underlying trichome development, we compared the transcriptomes of three mock-treated and three *ThMYBML2* VIGS lines by RNA-seq (refer to Fig. 4). To further validate the RNAseq results, we analyzed expression counts for our gene of interest as well as for genes known to have ubiquitous and stable expression (housekeeping genes). TRV2-*ML2* lines exhibited a four-fold decrease in *ThMYBML2* expression compared to mock controls, while the transcripts of the housekeeping genes *EEF1-alpha*, *Actin*, *Tubulin/FtsZ*, and *Ubiquitin-12* showed comparable expression levels in both treatments, as expected (Fig. 10a).

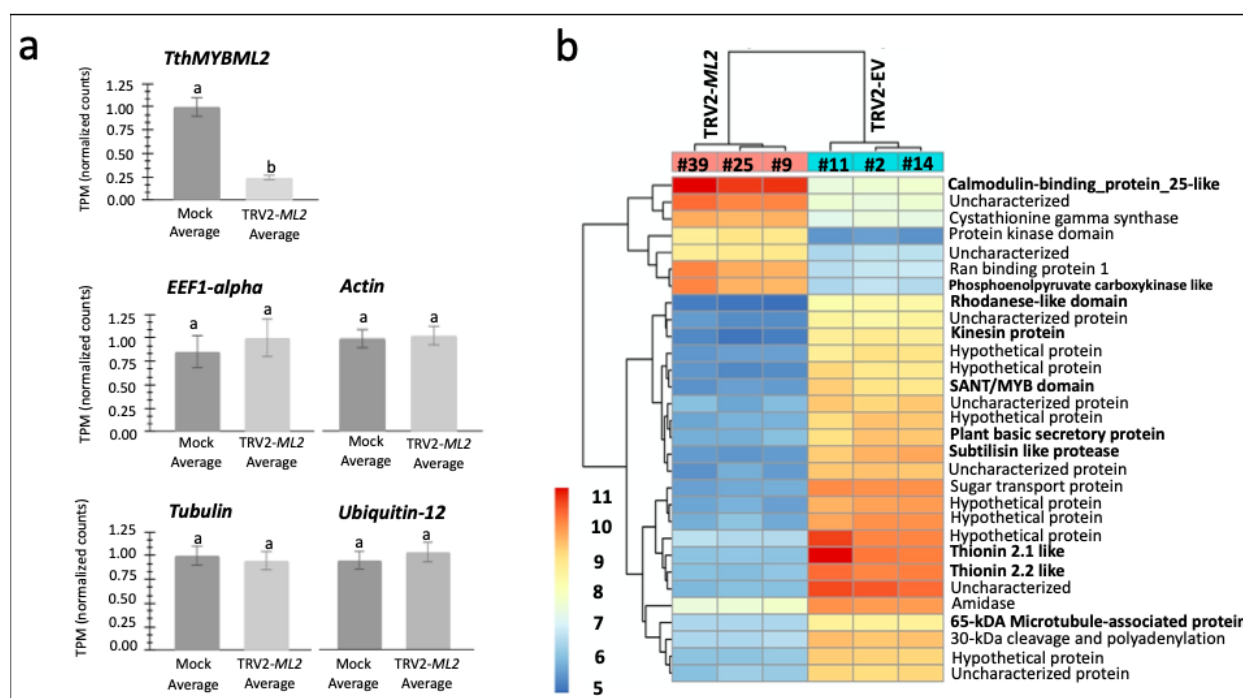


Figure. 10: Identification of candidates in the *Thalictrum MIXTA-like* regulatory gene network. RNAseq analysis of differentially expressed genes (DEGs) in leaves from plants targeted for *TthMYBML2* downregulation vs. empty vector controls (EV=mock-treated). (a) Validation of RNAseq: TPM normalized count expression of *TthMYBML2* in mock treated versus TRV2-*ML2*

transgenic lines shows that the targeted gene has significantly lower expression than controls, *while* four common housekeeping genes have comparable expression levels. Means \pm SE from three biological replicates, a different letter indicates a statistically significant difference ($p < 0.0001$) in a one-way ANOVA followed by Tukey's multiple comparisons. (b) Hierarchical clustering and heat-map of the top 30 DEGs with the highest or the lowest expression profiles, sorted by their adjusted p-values. The color scale indicates the expression levels (log₂-fold change) relative to the mock treated samples, with three biological replicates per treatment group (transgenic line numbers used for RNA-seq in bold, refer to Fig. 4b). Genes in bold are further discussed in the text. TPM= transcripts per million.

RNAseq analysis revealed approximately equal numbers of significant differentially expressed genes (DEGs) either upregulated (49%) or downregulated (50.3%) with a cut-off log₂-fold change ≥ 4 and ≤ -4 . Our functional annotation of the thirty highest and lowest expressing DEGs (Fig. 10b) revealed upregulation of a microtubule regulating calmodulin-binding protein (Oppenheimer et al., 1997) and a gluconeogenesis-associated Phosphoenolpyruvate carboxy-kinase like protein (Leegood et al., 2003). Downregulated candidates included motor proteins such as kinesin and 65 k-DA microtubule-associated protein (Reddy et al., 2004), defense and detoxification proteins such as Thionin 2.1/2 like (Escudero-Martinez et al., 2017) and Rhodanese-like domain protein, in addition to epidermal specific subtilisin-like protease (Groll et al., 2002), and SANT/MYB domain protein.

In *Arabidopsis*, calmodulin-like proteins interact with kinesin-microtubule motor proteins to regulate trichome morphogenesis (Oppenheimer et al., 1997, Reddy et al., 2004). Glandular trichomes of *Artemisia annua* secrete Rhodanese-like domain protein for defense and detoxification (Wu et al., 2012), while leaf specific-thionins are small metabolites with roles in plant defense against pathogens and herbivores (Escudero-Martinez et al., 2017). In terms of epidermal function, subtilisin-like proteases play a role in cell-to-cell signaling and spacing of

stomatal cells in plants (Groll et al., 2002); however, their role in the spacing of other epidermal cells is unknown. Hierarchical clustering of DEGs also revealed downregulation of a SANT/MYB DNA binding protein; a constituent of chromatin remodeling proteins (Boyer et al., 2004).

Discussion

Evolutionary history of *Thalictrum MIXTA-like*

Thalictrum is an early-diverging basal eudicot, a member of the Ranunculales, an order that is sister to the rest of the eudicot clade. Since *MIXTA* orthologs are exclusively found within the core eudicots, *Thalictrum* orthologs represent a “paleo” *MIXTA-like* lineage (Fig. 1a), analogous to how the APETALA3 subfamily of MADS-box genes has a paleoAP3 lineage in early diverging eudicots (Kramer 2001).

Phylogenetic inference of the *MIXTA-like* family in *Thalictrum* revealed a lineage-specific duplication that coincides with a WGD event in the genus (Di Stilio et al., 2021 *in prep*; Soza et al., 2013). This suggests that the evolution of the *MIXTA-like* gene family was impacted by polyploidy, which is ubiquitous in *Thalictrum*, early in the history of the genus.

T. thalictroides MIXTA-like is a positive regulator of leaf trichomes

Plants adapt to the external environment through sophisticated epidermal features, which can be used as morphological markers of organ and tissue types. In *T. thalictroides*, the MYB family R2R3 *MIXTA-like* gene was known to play a role in the development of conical cells in floral organs, constituting a micro-morphological marker of petaloidy connected to insect-pollination in the genus (Di Stilio et al., 2009). Through complementary functional approaches, this study has uncovered a novel role for *TthMYBML2* in leaves, as a positive regulator of trichome elongation, development, and density. Most subgroup 9-a *MIXTA-like* genes such as *Antirrhinum majus* AmMYBML1 (Perez Rodriguez et al., 2005) and *A. annua* AaMIXTA1 (Shi et al., 2018) are

positive regulators of trichome development. However, some *MIXTA-like* genes have developed inhibitory roles on trichome initiation, such as *Mimulus guttatus* *MgMYBML8* (Scoville et al., 2011) and *Arabidopsis* *MYB106* (Gilding and Marks, 2019). Since *Thalictrum* *MIXTA-like* genes belong to an early diverging eudicot sister clade to the core eudicot clade (Fig. 1a), they potentially provide a glimpse into the ancestral functions of paleo *MIXTA-like* orthologs. Our data hence suggests that the negative role of *MIXTA-like* genes in trichome development is a derived function specific to the core eudicots.

***Thalictrum* MIXTA-like modulates trichome morphogenesis via microtubule remodeling**

In recent years, *Arabidopsis* has become a model for studying the morphogenesis and anisotropic development of epidermal cells (Yang et al., 2019). Microtubule binding proteins, a component of the plant cytoskeleton, have been implicated in the development of both conical cells and branched trichomes (Reddy et al., 2004). Previously, trichomes with short stalks were observed in *Arabidopsis* loss of function mutants for Kinesin-like calmodulin-binding protein (KCBP) (Oppenheimer et al., 1997). However, the mechanism of trichome morphogenesis in species outside of this model plant is currently unknown. Our RNAseq data shows downregulation of a Kinesin protein, 65kDA microtubule-associated protein, and upregulation of the Calmodulin-binding protein 25-like. These results suggest that *MIXTA-like* orthologs from phylogenetically distant plant species regulate cell elongation using similar genetic components, pointing to the potential conservation of genetic machinery in the development of epidermal forms.

***Thalictrum* trichomes in plant defense**

Thalictrum species are cultivated for their wealth of biochemical compounds such as alkaloids found in roots and leaves (Hao et al, 2021). To the best of my knowledge, *Thalictrum* trichomes,

however, have not been evaluated before in terms of their ability to synthesize or accumulate bio-compounds. This study revealed that *ThMYBML2* silencing impacts trichome morphology, and affects genes related to stress, detoxification, and defense. Basic secretory protein (BSP), Rhodanese-like domain and Thionin-like proteins were co-repressed in transgenic plants undergoing gene silencing. Since thionins are markers of herbivore-induced systemic response (Escudero-Martinez et al., 2017), it appears likely that *Thalictrum* trichomes play a role in defense against herbivores. These same proteins are also known for their potential in anti-cancer therapeutics (Wang et al., 2007, Guzmán-Rodríguez et al., 2015).

MIXTA-like function in stigmatic papillae and pollination syndromes in *Thalictrum*

We explored the expression patterns of *MIXTA-like* homologs in species with variation in ploidy and stigma morphology in connection to pollination mode; capitate stigmas in insect pollinated species (*T. thalictroides*, 2X), or elongated, feathery stigmas in two wind-pollinated species (*T. dioicum* (4X) and *T. dasycarpum* (21X)). Our hypothesis was that since *MIXTA-like* genes trigger cell elongation, higher expression of *MIXTA-like* homologs would be found in carpels from wind-pollinated species due to their elongated stigmatic surfaces. Our results showed higher gene expression in carpels compared to other tissues, and this was consistent across the three species analyzed. However, wind-pollinated polyploid species showed paralog-specific expression, where both copies were expressed redundantly in *T. dioicum*, while one paralog showed specialization in *T. dasycarpum*. This result suggests that a gene dosage effect in stigmatic cell elongation might be present in the low level polyploid, whereas paralog specialization is more likely to occur at higher ploidy levels. In this study, I newly show that overexpression of *T. thalictroides* *MIXTA-like* gene i has a positive effect on stigmatic cell elongation. Therefore, future directions should include paralog-specific targeted silencing and in situ hybridization of *MIXTA-like* genes in representative species such as these, with contrasting flower morphologies, to further test this hypothesis.

How do *MIXTA-like* genes regulate the development of multiple, distinct epidermal forms, in different plant systems?

Previously, it has been speculated that timing, developmental stage, or localization may determine the specialized cell forms that develop from *MIXTA-like* expression (Perez Rodriguez, 2005). Interestingly, our comparative transcriptomic data revealed that *Thalictrum MIXTA-like* positively regulates a SANT/MYB domain containing protein involved in local chromatin remodeling (Boyer et al., 2002), suggesting that *MIXTA-like* genes could potentially regulate chromatin remodeling complexes to reprogram epidermal cell fate.

Functional studies of *MIXTA-like* orthologs in the monocot and core eudicot clades suggest that they are sufficient to drive the development of multiple, distinct epidermal features. For instance, in the orchid *P. aphrodite*, both *MIXTA-like* paralogs, *PaMYB9A1/2*, can drive the differentiation of conical cells and cuticle biosynthesis in petals (Lu et al., 2021). Similarly, snapdragon *AmMYBML1* can modulate the differentiation of trichomes in leaves and of conical cells in petals (Perez- Rodriguez et al., 2005). In the liverwort *Marchantia polymorpha* (a bryophyte), *MIXTA* homologs play a role in cuticle and papillate cells, representing a more ancestral function potentially common to all land plants (Xu et al., 2020). Here, we show that the *Thalictrum MIXTA-like* ortholog can modulate the differentiation and elongation of leaf trichomes, and previously floral conical cells. Hence, our results extend these functions to the early-diverging eudicots, allowing us to infer them back to at least the common ancestor of monocots and eudicots. . An interesting novel role was newly uncovered in stigmatic papillae in this study that warrants further investigation in the context of the different types of stigmas found in insect- and wind-pollinated flowers. In closing, these findings suggest a deeply conserved role in plant epidermis for these genes in flowering plants, where *MIXTA-like* transcription factors appear to have been co-opted to produce distinct epidermal forms.

Methods

Infiltration

The infiltration of *T. thalictroides* occurred as previously described (see Di Stilio et al., 2010) with modification. Briefly, TRV1, TRV2-*ML2*, and TRV2-*PDS-ML2* starter cultures were grown overnight with selective antibiotics and subsequently used to inoculate 500 ml cultures.

Agrobacterium were centrifuged at 4°C and 4,000g for 15 min before being resuspended in an infiltration medium (10 mM MES, 20 µM acetosyringone, and 10 mM MgCl₂). Each culture was resuspended to a final OD₆₀₀ of 2.0 and incubated for 3 hrs at room temperature. Silwet L-77 (Lehle Seeds, Round Rock, TX) was added 100 µL/L as a surfactant.

The dormant *T. thalictroides* tubers were kept in the cold 4C for 3 weeks, and a small razor blade incision was made about 1 cm from the meristem before being submerged in an infiltration medium containing a 1:1 ratio of TRV1 and TRV2 specific construct. *T. thalictroides* tubers were either treated with a construct with the gene of interest (TRV-*ML2*) alone, or with the marker gene Phytoene Desaturase (TRV-*PDS-ML2*) whose down regulation induces photobleaching. Forty-five tubers per treatment were vacuum infiltrated and potted in 2.5" Deepots™ (Stuewe & sons, Tangent, OR) using Sunshine Mix #4 soil (Sun Gro, Bellevue, WA). Plants were kept in growth chambers with the following conditions (16hr light-dark cycle, 22°C/18°C). As a negative control, fifteen untreated plants were grown under the same greenhouse conditions. An additional thirty-five mock treatment plants were infiltrated but the TRV2-EV did not contain an insert. This control was used to test for background viral effects.

Detection of viral transcripts by reverse transcriptase (RT) PCR

Fully expanded mature leaves were collected from plants 3-4 weeks post infiltration, flash-frozen with liquid nitrogen and stored at -80 °C. Total RNA was extracted using the

Spectrum Plant Total RNA Kit or Trizol reagent (Invitrogen, California, USA) according to the manufacturers extraction protocol. Samples were treated with DNase I and first-strand cDNA was synthesized using iScript cDNA synthesis kit. The primers used for cDNA synthesis were TRV1 and TRV2 specific (See Suppl. Table. 1 for full details). The cDNA was synthesized using the reverse primers OYL 198 and pYL156 R and amplified using a 51x30 PCR cycle. The RT-PCR products were run on 1.2% agarose gel and photographed on Bio-Rad Image lab software.

Gene expression analysis by real-time quantitative PCR (qPCR)

For paralog-specific expression, locus-specific primers were designed for each paralog using the Primer3 tool from NCBI. Quantification of expression for *T.thML2*, *TthPDS*, *T. dioML1*, *T. dioML2*, *T. dasML1*, *T. dasML2*, *T.dasML3*, *T.dasML4* was performed using qPCR, as previously described (Galimba et al., 2012). Briefly, each 10 μ l reaction contained 5 μ l of SYBR Green PCR Master Mix (Bio-Rad), 0.5 μ l (10 μ M) of locus-specific primers (Suppl. Table. 1), 1 μ l of template cDNA and 3 μ l of water. Samples were amplified for 40 cycles in duplicate, including a no-template control. Reactions were normalized to the *Thalictrum* orthologs of two housekeeping genes, *ACTIN* and *EEF1* (*EUKARYOTIC ELONGATION FACTOR 1*), using the Δ CT relative quantification method (Livak and Schmittgen, 2001). Standard deviation of Ct values of reference genes were calculated and average of technical replicates was used to ensure minimal variation in gene expression; Average values and standard errors were graphed and compared statistically by single factor Anova followed by Tukey's comparisons. All primers used in qRT-PCR with annealing temperatures are provided in the supplementary table.

Preparation of samples for Scanning electron microscopy (SEM)

Fully expanded, mature leaves were dissected and fixed in formaldehyde acetic acid-alcohol (FAA) for 1 hour at RT and overnight at 4°C, dehydrated through an alcohol series (50, 60, 70,

80, 95, and 100%), critical point dried, mounted on stubs and sputter coated with gold. Observations were made on the JEOL NeoScope JCM-7000 at the UW microscopy facility. Leaves fixed in FAA from an earlier tobacco bioassay overexpressing *TthMYBML2* under a strong constitutive promoter were prepared for SEM as previously described (Di Stilio et al. 2009).

Phenotyping of epidermal features

T. thalictroides leaves were imaged top, middle, and base on the adaxial and abaxial side. On the abaxial side, stomatal density was counted 1mm^2 adjacent to the mid vein. Trichomes were found only on the abaxial side, and were measured from the base to the tip using software Image J using either a straight or segmented line (n=41).

Trichomes in tobacco leaves were sampled from the abaxial and adaxial leaf sides, measurements were taken at the base of the leaf, 5mm^2 adjacent to the mid vein on both sides and averaged, the number of trichomes found for each type was averaged per treatment (n=4 independent lines per treatment). Significance was determined using a Two-factor ANOVA followed by bonferroni correction for multiple comparisons. To remove redundancy, chimeric trichomes were counted separately. For stigmatic papillae, regions clear of exudate were sampled. Measurements were taken from the waist to the tip in micrometers using the ImageJ straight or segmented line too (n=145). A two-tailed unpaired t-test was used to assess statistical significance.

Phylogenetic analysis of *Thalictrum MIXTA-like* genes

MIXTA-like homologs were recovered from all representative clades of the *Thalictrum* phylogeny, using either subcloning (TA cloning) and/or several sequencing primer sets. For species where colonies were sequenced, a minimum of 8 colonies for diploid species and 15 colonies for tetraploid species were used to recover all possible homologs. Sequences were

edited in Sequencher version 4.9 (Gene Codes Corporation, Ann Arbor, MI) and aligned using MUSCLE (Edgar, 2004). The sequences that were added after construction of a basic alignment were edited manually in UGENE. INDELS were coded as gaps '-' and missing data was coded as '?'s for all taxa. Models of evolution for each data set were determined using jModelTest version 2.1 (Posada, 2008). The model selected under the Akaike Information Criterion (Akaike 1974) was the GTR+I+ Γ model. Bayesian Inference analysis was conducted using MrBayes v.3.2 (Ronquist et al., 2012) with parallel MCMC analysis of 50 million generations, sampling every 1000 generations. Convergence was checked using the average standard deviation of split frequencies (<0.01) and the effective sample size (ESS) values (>200). The first 25% of trees were discarded as burn-in. The remaining trees were pooled to construct a 50% majority rule consensus tree and visualized using FigTree versions v1.4.4 (Rambaut, 2018).

Comparative transcriptomic analysis (RNAseq)

Four biological samples were collected and validated from mock treated and *TRV:ml2* treated lines, their total RNA was extracted for RNA-seq analysis. Sequencing was entrusted to the Genewiz facility, where Agilent 2100 Bioanalyzer (Agilent Technologies, Inc., CA, USA) and Qubit 2.0 were utilized to measure the purity of samples for subsequent library preparation. mRNA sequencing was conducted using polyA selection, adapters were removed from sequence reads using Trimmomatic v.0.36. The resulting reads were mapped to *Thalictrum_thalictroides* reference genome available on ENSEMBL using the Bowtie2 aligner v.2.2.6. Unique hit counts were calculated using featureCounts from the subread package v.1.5.2.

Differential Gene Expression Analysis

Gene hit counts were used for downstream differential expression analysis (DEGs). DeSeq2 was utilized to generate normalized hit counts, a reliable method for comparison of gene

expression between the mock treated and treated groups of samples. The Wald test was used to generate p-values for statistical significance and log₂ fold changes to quantify expression change between the groups. The Benjamini-Hochberg test was used to generate adjusted p-values. Genes with adjusted p-values <0.05 and absolute log₂ fold change >1 or <-1 were regarded as differential expressed genes. Significant DEGs were functionally annotated, and transcripts of interest, such as *TthMYBML2* and stable reference genes, were fished out of the assemblies using BLAST. Normalized counts corresponding to the transcripts were used for graphing expression of the orthologs. Average expression for three bio-replicates was normalized to mock treated controls and significance was calculated using single-factor ANOVA and tukey's for multiple comparison.

References

- Akaike, H. (1974). A new look at the statistical model identification. *IEEE Transactions on Automatic Control*, 19(6), 716–723. <https://doi.org/10.1109/tac.1974.1100705>
- Bar, M., & Shtein, I. (2019). Plant trichomes and the biomechanics of defense in various systems, with Solanaceae as a model. *Botany*, 97(12), 651–660. <https://doi.org/10.1139/cjb-2019-0144>
- Baumann, K., Perez-Rodriguez, M., Bradley, D., Venail, J., Bailey, P., Jin, H., ... Martin, C. (2007). Control of cell and petal morphogenesis by R2R3 MYB transcription factors. *Development*, 134(9), 1691–1701. <https://doi.org/10.1242/dev.02836>
- Bhakuni, D. S., & Singh, R. S. (1982). The Alkaloids of *Thalictrum foliolosum*. *Journal of Natural Products*, 45(3), 252–255. <https://doi.org/10.1021/np50021a003>
- Boyer, L. A., Latek, R. R., & Peterson, C. L. (2004). The SANT domain: A unique histone-tail-binding module? *Nature Reviews Molecular Cell Biology*, 5(2), 158–163. <https://doi.org/10.1038/nrm1314>
- Brockington, S. F., Alvarez-Fernandez, R., Landis, J. B., Alcorn, K., Walker, R. H., Thomas, M. M., ... Glover, B. J. (2012). Evolutionary analysis of the MIXTA gene family highlights potential targets for the study of cellular differentiation. *Molecular Biology and Evolution*, 30(3), 526–540. <https://doi.org/10.1093/molbev/mss260>
- Cavallini-Speisser, Q., Morel, P., & Monniaux, M. (2021). Petal cellular identities. *Frontiers in Plant Science*, 12. <https://doi.org/10.3389/fpls.2021.745507>
- Chalvin, C., Drevensek, S., Gilard, F., Mauve, C., Chollet, C., Morin, H., ... Boualem, A. (2021). Sclareol and linalyl acetate are produced by glandular trichomes through the MEP pathway. *Horticulture Research*, 8(1). <https://doi.org/10.1038/s41438-021-00640-w>
- Cummings, M. P. (2004). FigTree. In the *Dictionary of Bioinformatics and Computational Biology*. Chichester, UK: John Wiley & Sons, Ltd. Retrieved from <http://dx.doi.org/10.1002/9780471650126.dob0904>
- Dai, X., Zhou, L., Zhang, W., Cai, L., Guo, H., Tian, H., ... Wang, S. (2016). A single amino acid substitution in the R3 domain of GLABRA1 leads to inhibition of trichome formation in *Arabidopsis* without affecting its interaction with GLABRA3. *Plant, Cell & Environment*, 39(4), 897–907. <https://doi.org/10.1111/pce.12695>

- Di Stilio, V. S., Kumar, R. A., Oddone, A. M., Tolkin, T. R., Salles, P., & McCarty, K. (2010). Virus-Induced gene silencing as a tool for comparative functional studies in thalictrum. *PLoS ONE*, 5(8), e12064. <https://doi.org/10.1371/journal.pone.0012064>
- Di Stilio, V. S., Martin, C., Schulfer, A. F., & Connelly, C. F. (2009). An ortholog of MIXTA-like2 controls epidermal cell shape in flowers of *Thalictrum*. *New Phytologist*, 183(3), 718–728. <https://doi.org/10.1111/j.1469-8137.2009.02945.x>
- Edgar, R. C. (2004). MUSCLE: Multiple sequence alignment with high accuracy and high throughput. *Nucleic Acids Research*, 32(5), 1792–1797. <https://doi.org/10.1093/nar/gkh340>
- Escudero-Martinez, C. M., Morris, J. A., Hedley, P. E., & Bos, J. I. B. (2017). Barley transcriptome analyses upon interaction with different aphid species identify thionins contributing to resistance. *Plant, Cell & Environment*, 40(11), 2628–2643. <https://doi.org/10.1111/pce.12979>
- Feng, Z., Bartholomew, E. S., Liu, Z., Cui, Y., Dong, Y., Li, S., ... Liu, X. (2021). Glandular trichomes: New focus on horticultural crops. *Horticulture Research*, 8(1). <https://doi.org/10.1038/s41438-021-00592-1>
- Galdon-Armero, J., Arce-Rodríguez, L., Downie, M., Li, J., & Martin, C. (2020). A scanning electron micrograph-based resource for identification of loci involved in epidermal development in tomato: Elucidation of a new function for the mixta-like transcription factor in leaves. *The Plant Cell*, 32(5), 1414–1433. <https://doi.org/10.1105/tpc.20.00127>
- Gao, S., Gao, Y., Xiong, C., Yu, G., Chang, J., Yang, Q., ... Ye, Z. (2017). The tomato B-type cyclin gene, SlCycB2, plays key roles in reproductive organ development, trichome initiation, terpenoids biosynthesis and *Prodenia litura* defense. *Plant Science*, 262, 103–114. <https://doi.org/10.1016/j.plantsci.2017.05.006>
- Gao, S., Li, N., Niran, J., Wang, F., Yin, Y., Yu, C., ... Yao, M. (2021). Transcriptome profiling of *Capsicum annuum* using Illumina- and PacBio SMRT-based RNA-Seq for in-depth understanding of genes involved in trichome formation. *Scientific Reports*, 11(1). <https://doi.org/10.1038/s41598-021-89619-0>
- Guzmán-Rodríguez, J. J., Ochoa-Zarzosa, A., López-Gómez, R., & López-Meza, J. E. (2015). Plant antimicrobial peptides as potential anticancer agents. *BioMed Research International*, 2015, 1–11. <https://doi.org/10.1155/2015/735087>
- Hao, D.-C., Li, P., Xiao, P.-G., & He, C.-N. (2021). Dissection of full-length transcriptome and metabolome of *Dichocarpum* (Ranunculaceae): Implications in evolution of specialized

- metabolism of Ranunculales medicinal plants. *PeerJ*, 9, e12428.
<https://doi.org/10.7717/peerj.12428>
- Hichri, I., Deluc, L., Barrieu, F., Bogs, J., Mahjoub, A., Regad, F., ... Lauvergeat, V. (2011). A single amino acid change within the R2 domain of the VvMYB5b transcription factor modulates affinity for protein partners and target promoters selectivity. *BMC Plant Biology*, 11(1). <https://doi.org/10.1186/1471-2229-11-117>
- Hiscock, S. J., & Allen, A. M. (2008). Diverse cell signalling pathways regulate pollen-stigma interactions: The search for consensus. *New Phytologist*, 179(2), 286–317.
<https://doi.org/10.1111/j.1469-8137.2008.02457.x>
- Jaffe, F. W., Tattersall, A., & Glover, B. J. (2007). A truncated MYB transcription factor from *Antirrhinum majus* regulates epidermal cell outgrowth. *Journal of Experimental Botany*, 58(6), 1515–1524. <https://doi.org/10.1093/jxb/erm020>
- Jakoby, M. J., Falkenhan, D., Mader, M. T., Brininstool, G., Wischnitzki, E., Platz, N., ... Schnittger, A. (2008). Transcriptional profiling of mature arabidopsis trichomes reveals that NOECK encodes the mixta-like transcriptional regulator MYB106. *Plant Physiology*, 148(3), 1583–1602. <https://doi.org/10.1104/pp.108.126979>
- Javelle, M., Vernoud, V., Rogowsky, P. M., & Ingram, G. C. (2010). Epidermis: The formation and functions of a fundamental plant tissue. *New Phytologist*, 189(1), 17–39.
<https://doi.org/10.1111/j.1469-8137.2010.03514.x>
- Kramer, E. M., Di Stilio, V. S., & Schlüter, P. M. (2003). Complex Patterns of Gene Duplication in the APETALA3 and PISTILLATA Lineages of the Ranunculaceae. *International Journal of Plant Sciences*, 164(1), 1–11. <https://doi.org/10.1086/344694>
- Lashbrooke, J. G., Adato, A., Lotan, O., Alkan, N., Tsimbalist, T., Rechav, K., ... Aharoni, A. (2015). The tomato mixta-like transcription factor coordinates fruit epidermis conical cell development and cuticular lipid biosynthesis and assembly. *Plant Physiology*, pp.01145.2015. <https://doi.org/10.1104/pp.15.01145>
- Lau, S.-E., Schwarzacher, T., Othman, R. Y., & Harikrishna, J. A. (2015). dsRNA silencing of an R2R3-MYB transcription factor affects flower cell shape in a *Dendrobium* hybrid. *BMC Plant Biology*, 15(1). <https://doi.org/10.1186/s12870-015-0577-3>
- Leegood, R. C., & Walker, R. P. (2003). Regulation and roles of phosphoenolpyruvate carboxykinase in plants. *Archives of Biochemistry and Biophysics*, 414(2), 204–210.
[https://doi.org/10.1016/s0003-9861\(03\)00093-6](https://doi.org/10.1016/s0003-9861(03)00093-6)

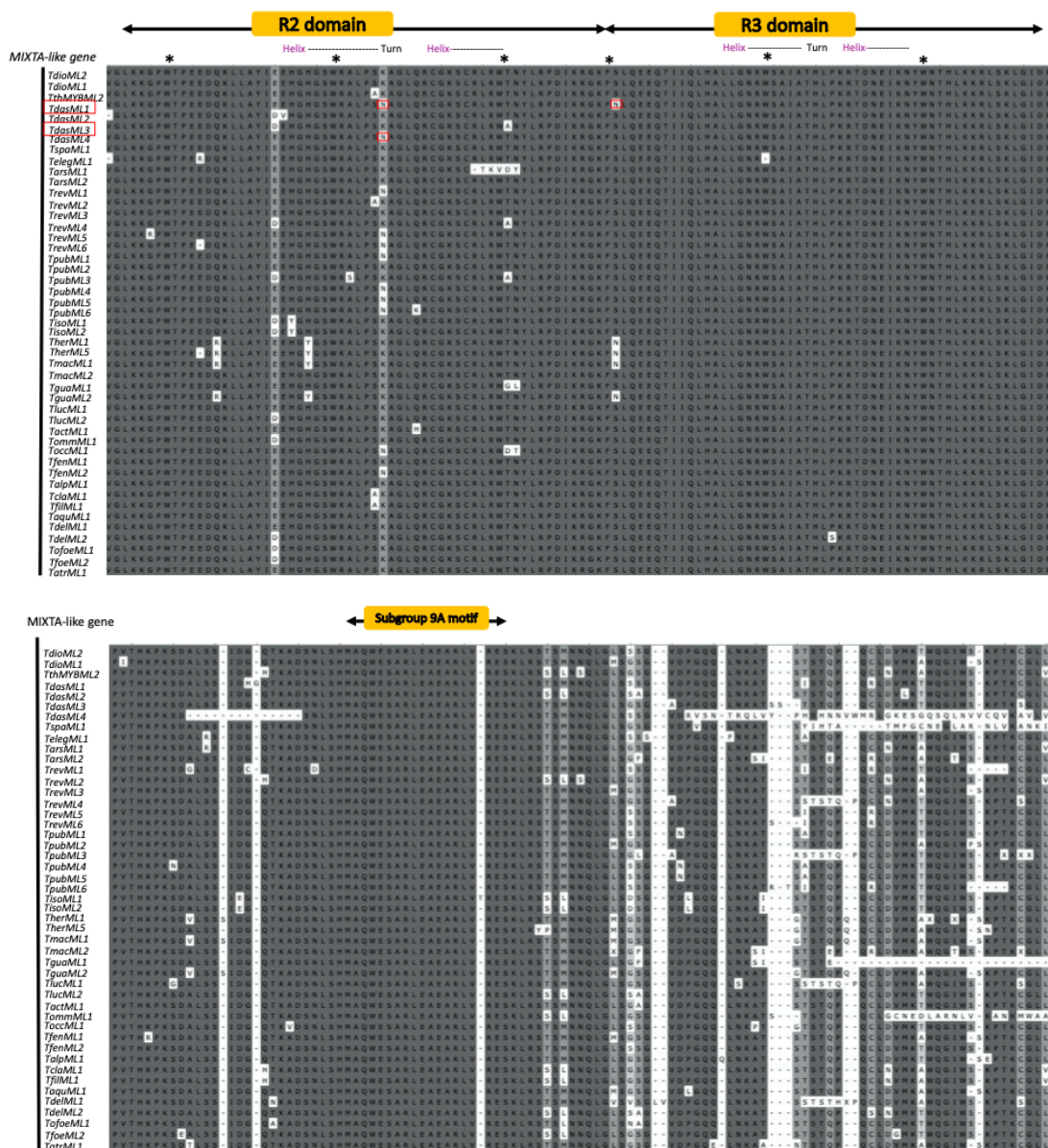
- Livak, K. J., & Schmittgen, T. D. (2001). Analysis of relative gene expression data using real-time quantitative PCR and the $2^{-\Delta\Delta CT}$ method. *Methods*, 25(4), 402–408. <https://doi.org/10.1006/meth.2001.1262>
- Lu, H.-C., Lam, S.-H., Zhang, D., Hsiao, Y.-Y., Li, B.-J., Niu, S.-C., ... Liu, Z.-J. (2021). R2R3-MYB genes coordinate conical cell development and cuticular wax biosynthesis in *Phalaenopsis aphrodite*. *Plant Physiology*. <https://doi.org/10.1093/plphys/kiab422>
- Machado, A., Wu, Y., Yang, Y., Llewellyn, D. J., & Dennis, E. S. (2009). The MYB transcription factor GhMYB25 regulates early fibre and trichome development. *The Plant Journal*, 59(1), 52–62. <https://doi.org/10.1111/j.1365-313x.2009.03847.x>
- Noda, K., Glover, B. J., Linstead, P., & Martin, C. (1994). Flower colour intensity depends on specialized cell shape controlled by a Myb-related transcription factor. *Nature*, 369(6482), 661–664. <https://doi.org/10.1038/369661a0>
- Oppenheimer, D. G., Pollock, M. A., Vacik, J., Szymanski, D. B., Ericson, B., Feldmann, K., & Marks, M. D. (1997). Essential role of a kinesin-like protein in *Arabidopsis* trichome morphogenesis. *Proceedings of the National Academy of Sciences*, 94(12), 6261–6266. <https://doi.org/10.1073/pnas.94.12.6261>
- Perez-Rodriguez, M., Jaffe, F. W., Butelli, E., Glover, B. J., & Martin, C. (2005). Development of three different cell types is associated with the activity of a specific MYB transcription factor in the ventral petal of *Antirrhinum majus* flowers. *Development*, 132(2), 359–370. <https://doi.org/10.1242/dev.01584>
- Pesch, M., & Hülskamp, M. (2009). One, two, three...models for trichome patterning in *Arabidopsis*? *Current Opinion in Plant Biology*, 12(5), 587–592. <https://doi.org/10.1016/j.pbi.2009.07.015>
- Plett, J. M., Wilkins, O., Campbell, M. M., Ralph, S. G., & Regan, S. (2010). Endogenous overexpression of *Populus* MYB186 increases trichome density, improves insect pest resistance, and impacts plant growth. *The Plant Journal*, 64(3), 419–432. <https://doi.org/10.1111/j.1365-313x.2010.04343.x>
- Posada, D. (2008). jModelTest: Phylogenetic Model Averaging. *Molecular Biology and Evolution*, 25(7), 1253–1256. <https://doi.org/10.1093/molbev/msn083>
- Qin, W., Xie, L., Li, Y., Liu, H., Fu, X., Chen, T., ... Tang, K. (2021). An R2R3-MYB Transcription Factor Positively Regulates the Glandular Secretory Trichome Initiation in *Artemisia annua* L. *Frontiers in Plant Science*, 12. <https://doi.org/10.3389/fpls.2021.657156>

- Reddy, V. S., Day, I. S., Thomas, T., & Reddy, A. S. N. (2003). KIC, a novel Ca^{2+} binding protein with one EF-hand motif, interacts with a microtubule motor protein and regulates trichome morphogenesis. *The Plant Cell*, *16*(1), 185–200. <https://doi.org/10.1105/tpc.016600>
- Ronquist, F., Teslenko, M., van der Mark, P., Ayres, D. L., Darling, A., Höhna, S., ... Huelsenbeck, J. P. (2012). MrBayes 3.2: Efficient bayesian phylogenetic inference and model choice across a large model space. *Systematic Biology*, *61*(3), 539–542. <https://doi.org/10.1093/sysbio/sys029>
- Scoville, A. G., Barnett, L. L., Bodbyl-Roels, S., Kelly, J. K., & Hileman, L. C. (2011). Differential regulation of a MYB transcription factor is correlated with transgenerational epigenetic inheritance of trichome density in *Mimulus guttatus*. *New Phytologist*, *191*(1), 251–263. <https://doi.org/10.1111/j.1469-8137.2011.03656.x>
- Soza, V. L., Haworth, K. L., & Di Stilio, V. S. (2013). Timing and consequences of recurrent polyploidy in meadow-rues (Thalictrum, Ranunculaceae). *Molecular Biology and Evolution*, *30*(8), 1940–1954. <https://doi.org/10.1093/molbev/mst101>
- Stracke, R., Holtgräwe, D., Schneider, J., Pucker, B., Rosleff Sørensen, T., & Weisshaar, B. (2014). Genome-wide identification and characterisation of R2R3-MYB genes in sugar beet (*Beta vulgaris*). *BMC Plant Biology*, *14*(1). <https://doi.org/10.1186/s12870-014-0249-8>
- Stracke, R., Werber, M., & Weisshaar, B. (2001). The R2R3-MYB gene family in *Arabidopsis thaliana*. *Current Opinion in Plant Biology*, *4*(5), 447–456. [https://doi.org/10.1016/s1369-5266\(00\)00199-0](https://doi.org/10.1016/s1369-5266(00)00199-0)
- Tian, J., Han, L., Feng, Z., Wang, G., Liu, W., Ma, Y., ... Kong, Z. (2015). Orchestration of microtubules and the actin cytoskeleton in trichome cell shape determination by a plant-unique kinesin. *ELife*, *4*. <https://doi.org/10.7554/elife.09351>
- Vashisth, A., Singh, D. K., Chakraborty, N., Purty, R. S., & Chatterjee, S. (2021). *Genome-Wide Study of the ABI3 Gene Family and Identification of Putative miRNA Targeting ABI3 Gene in Oryza Sativa ssp. Indica*. Research Square Platform LLC. Retrieved from Research Square Platform LLC website: <http://dx.doi.org/10.21203/rs.3.rs-749254/v1>
- Vernoud, V., Laigle, G., Rozier, F., Meeley, R. B., Perez, P., & Rogowsky, P. M. (2009). The HD-ZIP IV transcription factor OCL4 is necessary for trichome patterning and anther development in maize. *The Plant Journal*, *59*(6), 883–894. <https://doi.org/10.1111/j.1365-313x.2009.03916.x>

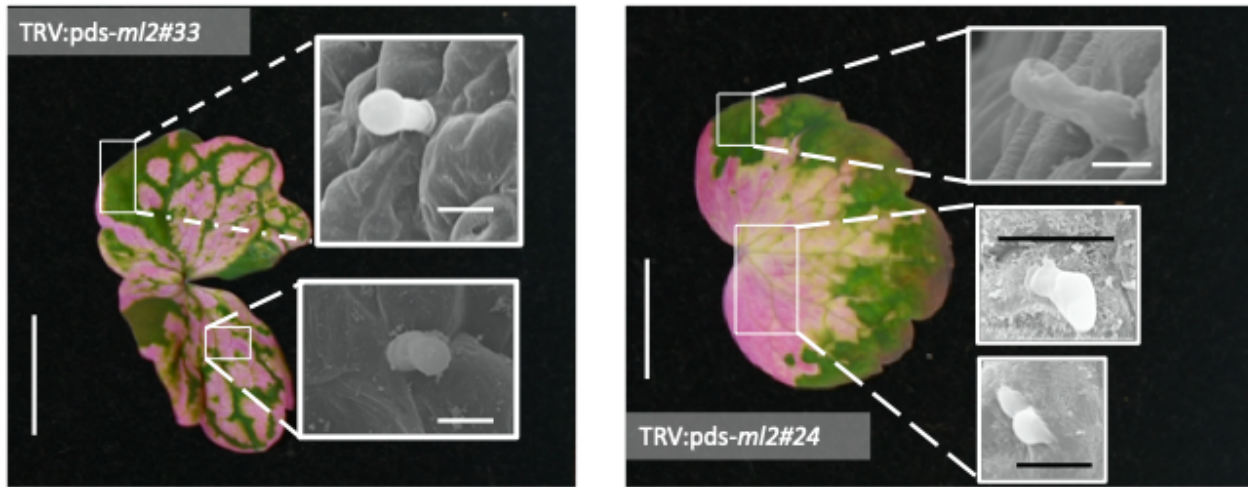
- von Groll, U., Berger, D., & Altmann, T. (2002). The subtilisin-like serine protease SDD1 mediates cell-to-cell signaling during arabidopsis stomatal development. *The Plant Cell*, *14*(7), 1527–1539. <https://doi.org/10.1105/tpc.001016>
- Walford, S.-A., Wu, Y., Llewellyn, D. J., & Dennis, E. S. (2011). GhMYB25-like: A key factor in early cotton fibre development. *The Plant Journal*, *65*(5), 785–797. <https://doi.org/10.1111/j.1365-313x.2010.04464.x>
- Wang, L., Allmann, S., Wu, J., & Baldwin, I. T. (2007). Comparisons of LIPOXYGENASE3- and JASMONATE-RESISTANT4/6-Silenced Plants Reveal That Jasmonic Acid and Jasmonic Acid-Amino Acid Conjugates Play Different Roles in Herbivore Resistance of *Nicotiana attenuata*. *Plant Physiology*, *146*(3), 904–915. <https://doi.org/10.1104/pp.107.109264>
- Wang, T. N., Clifford, M. R., Martínez-Gómez, J., Johnson, J. C., Riffell, J. A., & Di Stilio, V. S. (2018). Scent matters: Differential contribution of scent to insect response in flowers with insect vs. wind pollination traits. *Annals of Botany*, *123*(2), 289–301. <https://doi.org/10.1093/aob/mcy131>
- Wang, Y.-L., Nie, J., Chen, H.-M., Guo, C., Pan, J., He, H.-L., ... Cai, R. (2015). Identification and mapping of Tril, a homeodomain-leucine zipper gene involved in multicellular trichome initiation in *Cucumis sativus*. *Theoretical and Applied Genetics*, *129*(2), 305–316. <https://doi.org/10.1007/s00122-015-2628-4>
- Wu, J., Beal, J. L., & Doskotch, R. W. (1980). ChemInform abstract: ALKALOIDS OF THALICTRUM. 29. FOUR NEW THALIBRUNINE-RELATED ALKALOIDS FROM THALICTRUM ROCHEBRUNIANUM. *Chemischer Informationsdienst*, *11*(21). <https://doi.org/10.1002/chin.198021314>
- Wu, T., Wang, Y., & Guo, D. (2012). Investigation of Glandular Trichome Proteins in *Artemisia annua* L. Using Comparative Proteomics. *PLoS ONE*, *7*(8), e41822. <https://doi.org/10.1371/journal.pone.0041822>
- Xu, B., Taylor, L., Pucker, B., Feng, T., Glover, B. J., & Brockington, S. F. (2020). The land plant-specific MIXTA-MYB lineage is implicated in the early evolution of the plant cuticle and the colonization of land. *New Phytologist*, *229*(4), 2324–2338. <https://doi.org/10.1111/nph.16997>
- Yamada, K., Nagano, A. J., Nishina, M., Hara-Nishimura, I., & Nishimura, M. (2012). Identification of two novel endoplasmic reticulum body-specific integral membrane proteins. *Plant Physiology*, *161*(1), 108–120. <https://doi.org/10.1104/pp.112.207654>

- Yan, T., Li, L., Xie, L., Chen, M., Shen, Q., Pan, Q., ... Tang, K. (2018). A novel HD-ZIP IV/MIXTA complex promotes glandular trichome initiation and cuticle development in *Artemisia annua*. *New Phytologist*, *218*(2), 567–578. <https://doi.org/10.1111/nph.15005>
- Yang, C., & Ye, Z. (2012). Trichomes as models for studying plant cell differentiation. *Cellular and Molecular Life Sciences*, *70*(11), 1937–1948. <https://doi.org/10.1007/s00018-012-1147-6>
- Yang, Y., Huang, W., Wu, E., Lin, C., Chen, B., & Lin, D. (2019). Cortical microtubule organization during petal morphogenesis in arabidopsis. *International Journal of Molecular Sciences*, *20*(19), 4913. <https://doi.org/10.3390/ijms20194913>

Supplementary Materials



Suppl. Fig. 1: ClustalW amino acid alignment of R2R3 SBG9-A *MIXTA-like* genes from the genus *Thalicticum*. Conserved MYB domains R2,R3 and a Subgroup 9A domain are indicated, whereas the positions of helix-turn-helix regions are shown above the alignment. Dark grey shading indicates identity, light gray indicates similarity. Dashes indicate gaps; asterisks indicate conserved regularly spaced tryptophan residues.



Suppl. Fig. 2: Trichome phenotype in green and photobleached sectors of variegated leaves resulting from targeted silencing of *Thalictrum MIXTA* like. Insets show scanning electron microscopy of representative leaf trichomes in TRV2-*PDS-ML2* transgenic plants. Scale Bar= 10 mm (main panel), or 10 μ m (inset).

Suppl. Table 1. Summary of primers used in this study for VIGS validation (quantitative PCR) and cloning .

Primer Name	Sequence	Description
pTRV1_fwd=OYL195	5'-CTTGAAGAAGAAGACTTTTCGAAGTCTC-3'	TRV1 specific primer, RT PCR
pTRV1_rev=OYL198	5'-GTAAATCATTGATAACAACACAGACAAAAC-3'	TRV1 specific primer, RT PCR
qPCR_EEF-1alphaF4	5'-CTT CTT GCC TTC ACA CTT GGA GTC-3'	Housekeeping gene, RT qPCR
qPCR_EEF-1alphaR4	5'-TGT TGT CAC CCT CAA ACC CAG AG-3'	Housekeeping gene, RT qPCR
Tth Actin for2	5'-GCA GAA CGG GAA ATT GTC CGC-3'	Housekeeping gene, RT qPCR
Tth Actin rev2	5'-CCTGCAGCTTCCATTCCGATCA-3'	Housekeeping gene, RT qPCR
PYL156F	5'-GGTCAAGGTACGTAGTAGAG-3'	TRV2 specific primer, RT PCR
PYL156R	5'-CGAGAATGTCAATCTCGTAGG-3'	TRV2 specific primer, RT PCR
TthPDS_F_RT	5' - TGA ACA ACG ATG GAA CCG TG - 3'	<i>TthPDS</i> specific primer, RT qPCR
TthPDS_R_RT	5' - GTC AGC ATA CAC ACT CAA AAG G - 3'	<i>TthPDS</i> specific primer, RT qPCR
TthML2_qPCR_F3	5'-CAG TGA AAG AAG AAT GTG ATG AAG AGTA -3	TthML2 specific primer, RT qPCR
TthML2_qPCR_R3	5'-TGA CTG GAA TGT GCT CGT TTC-3'	<i>TthML2</i> specific primer RT qPCR
TdioT1F1_qpcr	5' TGA AGA GTA TAT GGG TGG TGG T -3'	<i>T.dioicum</i> ML2 copy1 specific primer, qPCR
TdioT1R1_qpcr	5' TTG GAT GAT TCT GAC GCC CA -3'	<i>T.dioicum</i> ML2 copy1 specific primer, qPCR
TdioT2F1_qpcr	5' GTT CCT CCT ATC ATT AAT AGA G -3'	<i>T.dioicum</i> ML2 copy2 specific primer, qPCR
TdioT2R1_qpcr	5' CAG AAT CAT CAT CAA AAG TTG GA -3'	<i>T.dioicum</i> ML2 copy2 specific primer, qPCR
TdasyT1F1_qpcr	5' GCT AAG CTC AAT TGA TCA CG -3'	<i>T.dasy carpum</i> ML2 copy1 specific primer, qPCR
TdasyT1R1_qpcr	5' CGT TGT GGC TGT GTG GAT A -3	<i>T.dasy carpum</i> ML2 copy1 specific primer, qPCR
TdasyT2F2_qpcr	5' AAG TTG CGG TCC AGT TCA TT -3'	<i>T.dasy carpum</i> ML2 copy2 specific primer, qPCR
TdasyT2R2_qpcr	5' TCA GAT CAA GCG AAG TCA TAG -3'	<i>T.dasy carpum</i> ML2 copy2 specific primer, qPCR
TdasyT3F1_qpcr	5' CTG GTC TGC TAA CAG GTG AAG GG -3'	<i>T.dasy carpum</i> ML2 copy3 specific primer, qPCR
TdasyT3R1_qpcr	5' AAC ACC TTC AGA AGT GCC TGA TGG -3'	<i>T.dasy carpum</i> ML2 copy3 specific primer, qPCR
TdasyT4F1_qpcr	5' CAG TAC TGG TGG TGG CCT TGA T -3'	<i>T.dasy carpum</i> ML2 copy4 specific primer, qPCR
TdasyT4R1_qpcr	5' GCA AAG GCA TAG GGT TAT CGC -3'	<i>T.dasy carpum</i> ML2 copy3 specific

		primer, qPCR
ML2ForDeg2	5' TCT CTT CTG CTT CAC CAC TTC -3'	Degenerate primers for <i>ML2</i> gene, cloning
ML2RevDeg2	5'ATT AAT KTG ATT GAG CTT GTC AGG T -3'	Degenerate primers for <i>ML2</i> gene, cloning
TthMYBML2_IntF	5'-TTC AGA GGT GTG GAA AGA GTT-3'	Used to close <i>ML2</i> internal gaps in gDNA, cloning
TthMYBML2_IntR2	5'-GCT TTG ACC AGR TTC CTT GC-3'	Used to close <i>ML2</i> internal gaps in gDNA, cloning